

# Experimental test on bridge jointed twin-towered buildings to stochastic wind loads

Z.-H. Ni<sup>†</sup>, C.-K. He<sup>‡</sup>, Z.-N. Xie<sup>‡†</sup>, B.-Q. Shi<sup>‡‡</sup> and D.-J. Chen<sup>‡‡</sup>

*Department of Civil Engineering, Shantou University, Shantou, Guangdong, 515063, P.R. China*

**Abstract.** This paper presents results of a study on wind loads and wind induced dynamic response of bridge jointed twin-towered buildings. Utilizing the high-frequency force balance technique, the drag and moment coefficients measured in wind tunnel tests, and the maximum acceleration rms values on the top floor of towers, are analyzed to examine the influence of building's plan shapes and of intervals between towers. The alongwind, acrosswind and torsional modal force spectra are investigated for generic bridge jointed twin-towered building models which cover twin squares, twin rhombuses, twin triangles, twin triangles with sharp corners cut off, twin rectangles and individual rectangle with the same outline aspect ratio as the twin rectangles. The analysis of the statistical correlation among three components of the aerodynamic force corroborated that the correlation between acrosswind and torsional forces is significant for bridge jointed twin-towered buildings.

**Key words:** twin-towered buildings; wind loads; wind-induced response; high-frequency force balance technique.

---

## 1. Introduction

Tall buildings constructed of high-strength and lightweight materials tend to be relatively flexible and lightly damped. Fluctuating wind loads on these tall buildings can cause excessive motion that may be disturbing to the occupants. Designers have now had to resort increasingly to dynamic analysis of buildings by means of wind tunnel testing. The high-frequency force balance may be used for determining the fluctuating wind load information from scale models of buildings which may be employed to obtain the dynamic response for a wide range of structural characteristics (Kareem 1992).

The bridge jointed twin-towered building is one of the new structural systems. The fundamental natural frequency of the sway vibration may be affected by the mass of the joint bridge, however, the first sway mode shape may still be considered a linear mode shape, which is the assumption for derivation of the force balance theory (Tschanz & Davenport 1983). The existence of the interval between towers renders the flow pattern around towers rather complicated. The velocity of the approach flow passing through the interval will be speeded up, which may disturb the vortex shedding and wake behind towers. Additionally, the aerodynamic loads acting on twin-towered buildings may be influenced by the plan shapes of twin towers. The object of this paper is to investigate the fluctuating wind induced structural loads and dynamic response of bridge jointed twin-towered buildings for a

---

<sup>†</sup> Professor

<sup>‡</sup> Graduate Student

<sup>‡†</sup> Associate Professor

<sup>‡‡</sup> Lecturer

range of different plan shapes using the high-frequency force balance technique.

## 2. Wind tunnel testing

### 2.1. Experimental equipment

The experiments were carried out in the wind tunnel laboratory of the Shantou University. The working section of the tunnel for building model tests is 20 m long, 3 m wide and 2 m high. The tests were conducted for the approach flow characteristics representing the urban exposure with the exponent of the power law profile being 0.20, and for different angles of the approach flow to examine the maximum of wind loads and response. The mean velocity profile and turbulence intensity distribution is shown in Fig. 1.

A high-frequency force balance with six components is made according to the suggestion from the force balance theory (Tschanz & Davenport 1983). Table 1 gives the design loads, the sensitivity and the natural frequency of the balance, where  $X$ ,  $Y$ , and  $Z$  are the drag, the vertical lift, and the transversal lift, respectively.  $M_x$ ,  $M_y$ , and  $M_z$  are the moments around the drag, the vertical lift and the transversal lift direction.

To ensure signals good accuracy the wind speed measured at the top of the building model during tests is chosen as 9 m/s. The HyScan 1000 data acquisition system and the module ZOCEIM16 are employed during all the acquisition. With the channel interval of 60  $\mu$ s and the channels number used of 8, the sampling rate is  $1/(60 \times 8)=2000$  Hz. The sampling duration is 2 seconds.

### 2.2. Outline of test models

A host of ultra-light models for generic bridge jointed twin-towered buildings with different plan

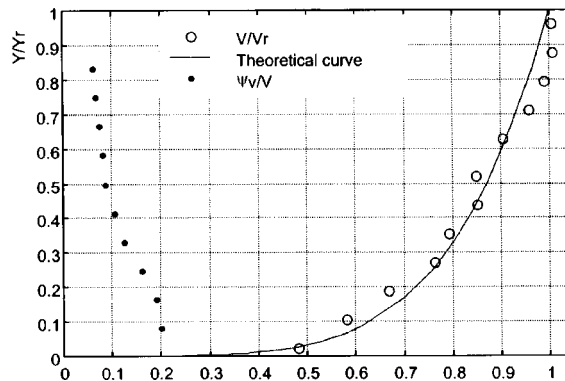


Fig. 1 Mean velocity and turbulence intensity profiles

Table 1 Parameters of force balance

	$X$	$Y$	$Z$	$M_x$	$M_y$	$M_z$
Natural frequency (Hz)	404	136	146	236	1064	240
Sensitivity (g)	0.38	0.5	0.3	0.3	0.3	0.3
Design load (N or N·m)	19.6	9.8	9.8	1.47	0.98	1.47

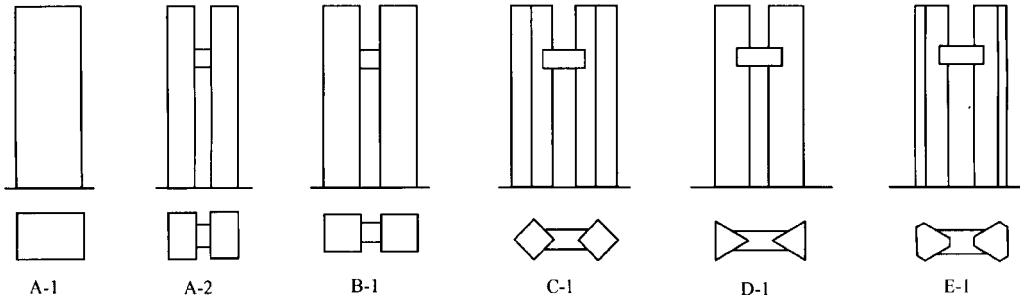


Fig. 2 The front and plan views of models

shapes and different intervals between towers was fabricated (Fig. 2). The plan shapes of towers cover individual rectangle labeled as A-1, twin rectangles labeled as A-2 with the same outline aspect ratio as A-1, twin squares, twin rhombuses, twin triangles, and twin triangles with sharp corners cut off. The later four models are labeled as B-1, C-1, D-1 and E-1, respectively, where the suffix “-1” denotes 11 m of the distance between two walls or two edges of towers for the prototypes. Other correspondent four models are labeled as B-2, C-2, D-2 and E-2, respectively, with the distance above being 15 m for the prototypes.

All the ten models are made of candlenut wood which has lightweight and enough rigidity. The cross section area of the prototype A-1 is  $56 \times 37.5$  m. Each side of the square of the prototype B is 30 m. Each side of the rhombus of the prototype C is 22.5 m. Each side of the triangle of the prototype D is 25 m, and for the prototype E a small triangle with each side being 3.5 m is cut off from each corner of the big triangle. The bridge connected two towers is 110 m high above the ground for all prototypes. With the lightweight of models the natural frequency of the system composed of the balance and model is about 40 Hz for the drag direction.

The geometric scale of all the ten models to prototypes is 1:375 with prototypes standing 150 m high. In estimating the response of buildings, the fundamental frequencies of the two sway mode and torsion mode for prototypes are taken to be  $n_x = 0.32$  Hz,  $n_z = 0.4$  Hz and  $n_\theta = 0.4$  Hz, respectively, where  $x$  is the direction perpendicular to the joint bridge and  $z$  is the direction along the joint bridge. The mass density of buildings is taken to be  $190 \text{ kg/m}^3$ , and the modal damping ratio in the fundamental mode is taken to be 0.05. The design ten-minute mean wind speed for prototypes at 150 m height of the top level of buildings is defined as 45 m/s based on the ten-year return period wind velocity of Shenzhen district.

### 3. Aerodynamic loads

#### 3.1. Formulation

The power spectral density of the dynamic moment at the building base,  $M(t)$ , may be written

$$S_M(\omega) = \int_0^H \int_0^H S_w(\omega, y_1, y_2) y_1 y_2 dy_1 dy_2 \quad (1)$$

where  $y$  is the vertical axis, and  $S_w(\omega, y_1, y_2)$  is the cross power spectral density of the fluctuating wind load per unit height,  $w(t, y)$ , between heights  $y_1$  and  $y_2$ . Taking only the first vibration mode in each direction,  $\phi(y)$ , the power spectral density of the modal force,  $F(t)$ , is

$$S_F(\omega) = \int_0^H \int_0^H S_w(\omega, y_1, y_2) \phi(y_1) \phi(y_2) dy_1 dy_2 \quad (2)$$

in which

$$F(t) = \int_0^H w(t, y) \phi(y) dy \quad (3)$$

It is noticed that when the sway mode and torsion mode are taken to be  $\phi(y) = y/H$ ,  $\phi_\theta(y) = 1$ , respectively, the alongwind, acrosswind and torsional modal force spectra are obtained as follows

$$S_{F_x}(\omega) = \frac{S_{M_x}(\omega)}{H^2}, \quad S_{F_z}(\omega) = \frac{S_{M_x}(\omega)}{H^2}, \quad S_{F_\theta}(\omega) = S_{M_y}(\omega) \quad (4)$$

According to the modal expansion theory (Clough & Penzien 1993), the uncoupled modal equation of motion may be expressed as

$$\ddot{q}_j + 2\zeta_j \omega_j \dot{q}_j + \omega_j^2 q_j = \frac{1}{m_j} F_j(t) \quad (5)$$

in which  $q_j$ ,  $F_j(t)$ ,  $m_j$ ,  $\omega_j$ ,  $\zeta_j$  = the modal coordinate, modal force, modal mass, undamped natural frequency and modal damping ratio associated with the  $j$ th mode. Based on the random vibration theory, the power spectral densities of modal coordinates  $S_q(\omega)$  and modal forces  $S_F(\omega)$  are related by the matrix equation

$$S_q(\omega) = \mathbf{H}^*(\omega) S_F(\omega) \mathbf{H}(\omega) \quad (6)$$

in which  $\mathbf{H}(\omega)$  is the diagonal matrix of frequency response functions :

$$\mathbf{H}(\omega) = \mathbf{diag} [m_j^{-1}(\omega_j^2 - \omega^2 + i2\zeta_j \omega_j \omega)^{-1}] \quad (7)$$

and  $\mathbf{H}^*(\omega)$  = the complex conjugate of  $\mathbf{H}(\omega)$ . The correlation function matrices of modal displacements  $\mathbf{D}_q$ , and modal accelerations  $\mathbf{D}_{\ddot{q}}$ , are obtained by calculating the following integrals (Islam, Ellingwood and Corotis 1990).

$$\mathbf{D}_q = \int_0^\infty \mathbf{Re}[S_q(\omega)] d\omega \quad (8)$$

$$\mathbf{D}_{\ddot{q}} = \int_0^\infty \mathbf{Re}[\omega^4 S_q(\omega)] d\omega \quad (9)$$

where  $\mathbf{Re}[\ ]$  denotes the real part. The correlation function matrices of building displacements  $\mathbf{D}_U$ , and accelerations  $\mathbf{D}_{\ddot{v}}$  may be obtained by the relationship

$$\mathbf{D}_U = \Phi \mathbf{D}_q \Phi^T \quad (10)$$

$$\mathbf{D}_{\ddot{v}} = \Phi \mathbf{D}_{\ddot{q}} \Phi^T \quad (11)$$

where  $\Phi$  = modal matrix,  $\mathbf{U} = \{u^T, v^T, \theta^T\}^T$ ,  $u$ ,  $v$ ,  $\theta$  are the alongwind, acrosswind displacements and torsional angle displacement, respectively. The diagonal elements of  $\mathbf{D}_U$  and  $\mathbf{D}_{\ddot{v}}$  are the mean-square values of building displacements and accelerations. Since only the first mode in each direction was taken in the high-frequency force balance technique, Eq. (6) becomes

$$S_d(\omega) = m_1^{-2} [(\omega_1^2 - \omega^2)^2 + (2\zeta_1 \omega_1 \omega)^2]^{-1} S_F(\omega) \quad (12)$$

in which

$$m_1 = \int_0^H m(y) \phi^2(y) dy \quad (13)$$

is the modal mass and  $m(y)$  = mass density per unit height. For evaluating the torsional response,  $m(y)\gamma^2$  is employed instead of  $m(y)$  in the integral above, where  $\gamma$  = the inertia radius of building cross-section.

### 3.2. Wind load coefficients and rms acceleration

Utilizing a high-frequency force balance, the correlation functions of the alongwind, acrosswind and torsional components of the modal aerodynamic loads are quantified for all models. Using the FFT technique, the alongwind, acrosswind and torsional modal force spectra are obtained and used to calculate the maximum root mean square values of the displacement and acceleration on the top floor of towers. Table 2 gives the maximum of dynamic force coefficients which are defined as follows

$$c_{f_x} = \frac{\psi_{f_x}}{\frac{1}{2}\rho V_H^2 B H}, \quad c_{f_z} = \frac{\psi_{f_z}}{\frac{1}{2}\rho V_H^2 B H}, \quad c_{M_y} = \frac{\psi_{M_y}}{\frac{1}{2}\rho V_H^2 B^2 H} \quad (14)$$

where  $\rho$  = the density of air,  $V_H$  = the mean wind velocity at the height,  $H$ , of towers,  $B$  = the building characteristic width (the maximum dimension along the joint bridge),  $\psi$  = the rms value,  $f_x$ ,  $f_z$  = the drags along  $x$ ,  $z$  direction, respectively,  $M_y$  = the torsion moment about vertical axis  $y$ . Analogously, the static force coefficients are defined as follows

$$c_{sf_x} = \frac{\mu_{f_x}}{\frac{1}{2}\rho V_H^2 B H}, \quad c_{sf_z} = \frac{\mu_{f_z}}{\frac{1}{2}\rho V_H^2 B H}, \quad c_{sM_y} = \frac{\mu_{M_y}}{\frac{1}{2}\rho V_H^2 B^2 H} \quad (15)$$

in which  $\mu$  = the mean value,  $\rho$ ,  $V_H$ ,  $B$ ,  $H$  have the same meaning as the above.

The maximum rms accelerations on the top floor of towers are shown in Table 3 where the subscript  $\ddot{u}$ ,  $\ddot{v}$ , and  $\ddot{\theta}$  denote the alongwind, acrosswind and torsional acceleration, respectively. The mean square acceleration at the corner  $P(\hat{x}, \hat{z})$  which is farthest from the centre of section area on

Table 2 Maximum dynamic force coefficients

Models	$c_{f_x}$	$c_{f_z}$	$c_{M_y}$
A-1	0.109	0.116	0.019
A-2	0.105	0.105	0.045
B-1	0.057	0.038	0.021
B-2	0.082	0.041	0.028
C-1	0.065	0.041	0.015
C-2	0.083	0.044	0.012
D-1	0.105	0.071	0.027
D-2	0.096	0.068	0.036
E-1	0.089	0.063	0.031
E-2	0.101	0.064	0.040

Table 3 Maximum rms acceleration ( $m/s^2$  or  $rad/s^2$ ) on top floor

Models	$\Psi_{ii}$	$\Psi_{\dot{v}}$	$\Psi_{\dot{\theta}}$	$\Psi_p$
A-1	0.032	0.0082	0.00062	0.035
A-2	0.033	0.0135	0.00106	0.039
B-1	0.021	0.0080	0.00058	0.023
B-2	0.030	0.0077	0.00074	0.037
C-1	0.033	0.0103	0.00137	0.062
C-2	0.033	0.0117	0.00110	0.058
D-1	0.067	0.025	0.00115	0.069
D-2	0.072	0.024	0.00076	0.073
E-1	0.055	0.021	0.00072	0.056
E-2	0.068	0.023	0.00081	0.069

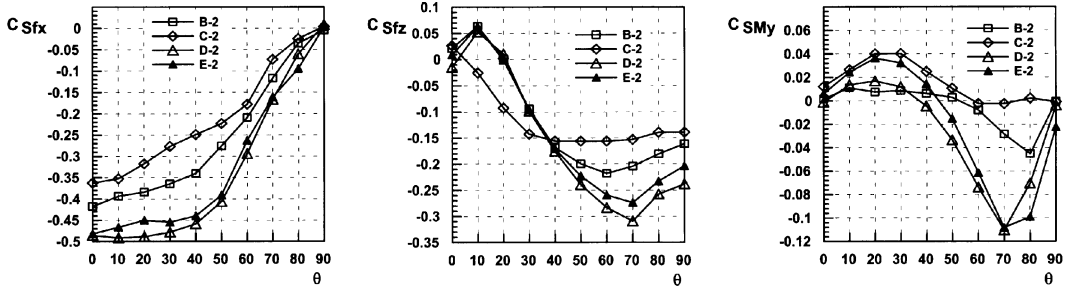


Fig. 3 Static force coefficients as functions of wind direction

the top floor is given approximately by (Islam, Ellingwood and Corotis 1990)

$$\Psi_p^2 = \Psi_{\ddot{u}}^2 + \Psi_{\dot{v}}^2 + (\hat{x}^2 + \hat{z}^2) \Psi_{\dot{\theta}}^2 + 2\hat{x}\Psi_{\ddot{u}\dot{\theta}} - 2\hat{z}\Psi_{\dot{v}\dot{\theta}} \quad (16)$$

where

$$\Psi_{\ddot{u}\dot{\theta}} = E[\ddot{u}(t)\dot{\theta}(t)], \quad \Psi_{\dot{v}\dot{\theta}} = E[\dot{v}(t)\dot{\theta}(t)] \quad (17)$$

It is noticed from the tables above that the maximum dynamic force coefficients, and maximum rms accelerations for most cases gained with the enlargement of the interval between towers within a range. So do the static force coefficients. By comparing data of building D and E it is found that both dynamic force coefficients and rms accelerations descended when sharp corners of the plan shape were cut off.

Fig. 3 shows the static drag coefficients and the static torsion moment coefficient as functions of wind direction  $\theta$ . It is observed that static drags acting on the building C are less than those on buildings B, D, E, and the static torsion moment acting on the building B is less than those on buildings C, D, E.

## 4. Wind force spectra

### 4.1. Wind load spectra

The alongwind, acrosswind and torsional modal force spectra for buildings labeled as A, C, D and E are shown in non-dimensional form in Fig. 4, Fig. 5, Fig. 6 and Fig. 7, respectively, where  $\theta = 0^\circ$

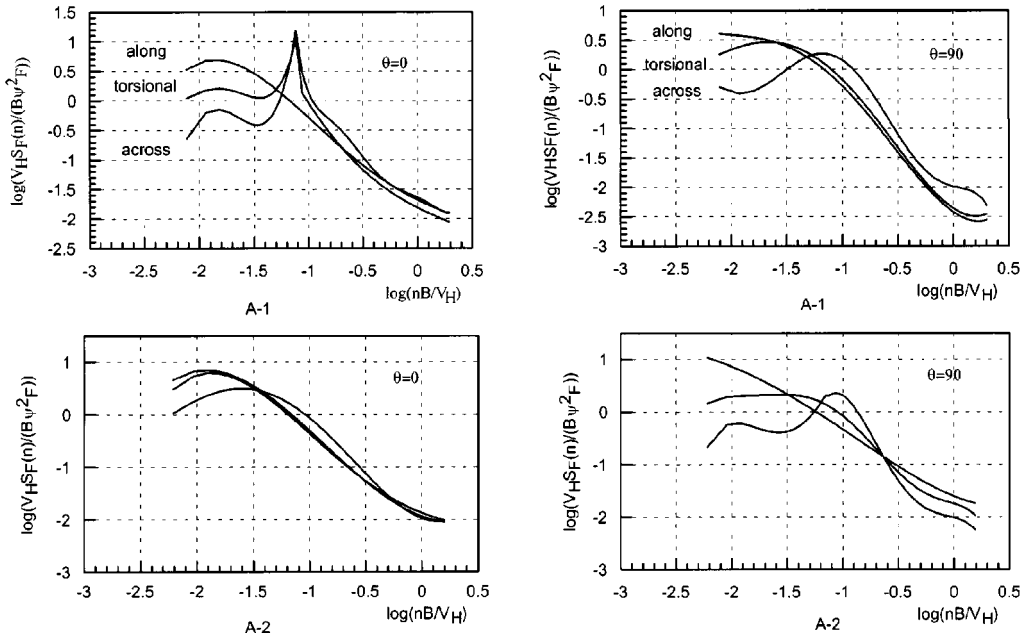


Fig. 4 Modal force spectra for building A

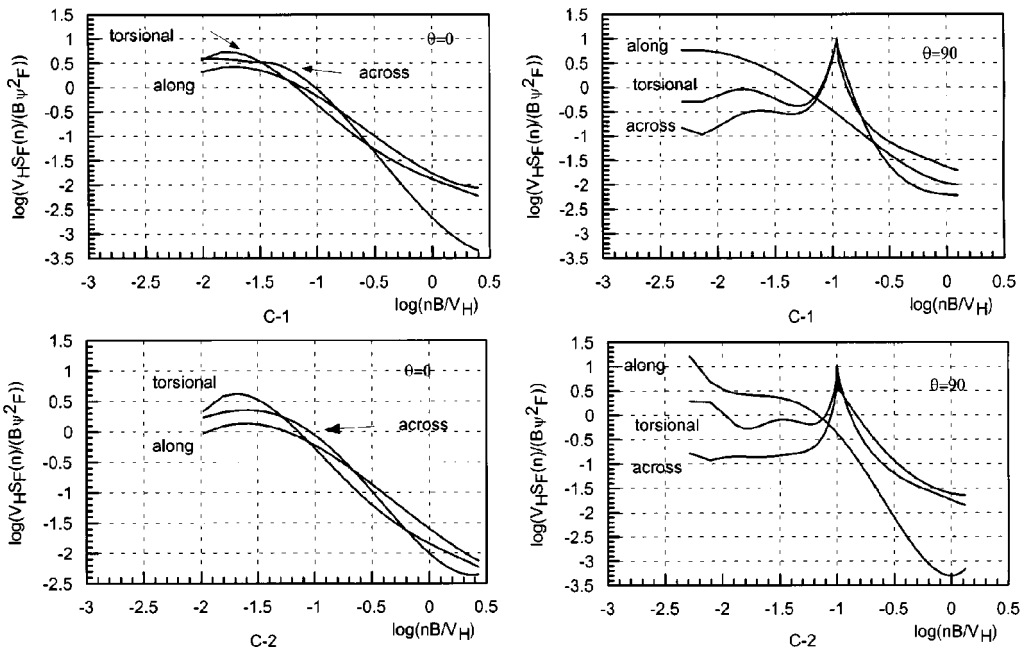


Fig. 5 Modal force spectra for building C

is the wind direction perpendicular to the joint bridge, and  $\theta = 90^\circ$  is the wind direction along the joint bridge. The abscissa in figures above is  $\log(nB / V_H)$  and the ordinate is  $\log(V_H S_F(n) / (B \psi_F^2))$  in which  $n$  = the frequency,  $S_F(n)$  = the wind modal force spectra,  $\psi_F^2$  = the mean square value of

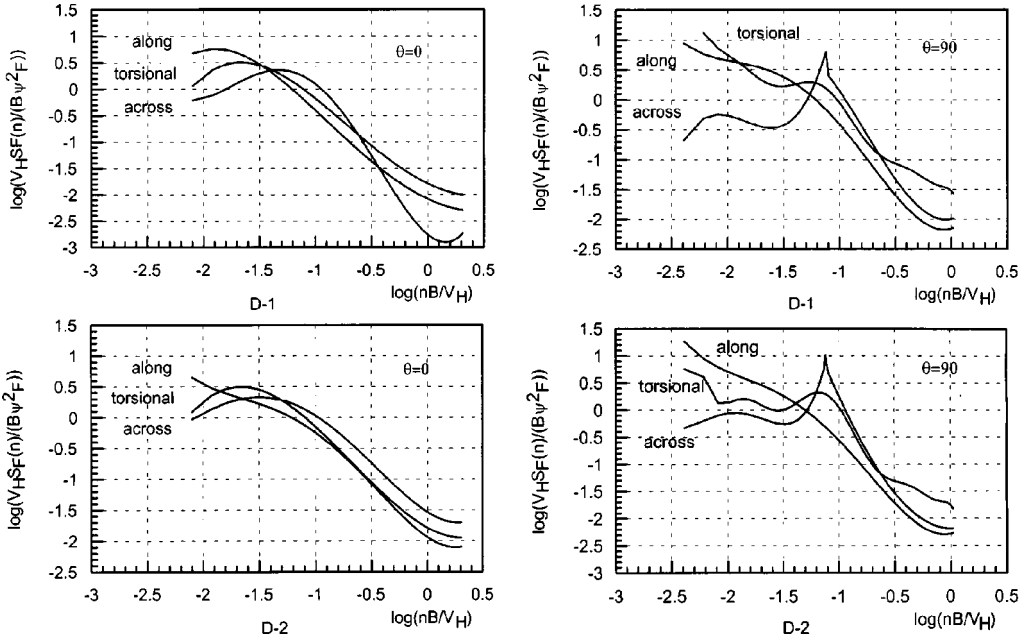


Fig. 6 Modal force spectra for building D

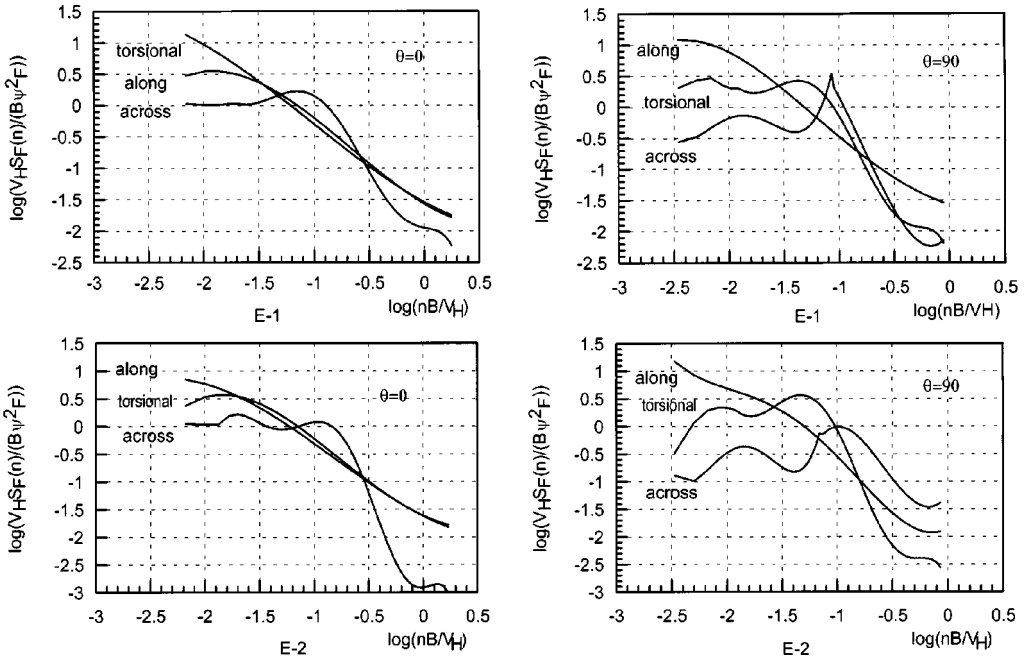


Fig. 7 Modal force spectra for building E

the modal force.

The alongwind force spectra in Fig. 4 are similar to wind gust spectra, suggesting that buffeting due to incident turbulence is the main cause of the force. When the approach flow is perpendicular

to the joint bridge (i.e.,  $\theta = 0^\circ$ ) the acrosswind and torsional force spectra for building A-1 show a pronounced peak at reduced frequency  $nB / V_H$  of about 0.08-0.10, which is near the Strouhal number of a square prism. These peaks represent the contribution of vortex shedding to the acrosswind and torsional forces. However, those peaks of acrosswind and torsional force spectra for building A-1 at  $\theta = 0^\circ$  disappeared for building A-2 at  $\theta = 0^\circ$ . It suggests that vortex shedding is no more the main contribution to acrosswind and torsional forces due to the distortion of the vortex street by the flow passing through the interval between two towers. When the approach flow is along the joint bridge (i.e.,  $\theta = 90^\circ$ ) the spectra for building A-2 resemble those for A-1, and the peaks of acrosswind spectra near  $nB / V_H \approx 0.1$  represent the contribution of vortex shedding again.

Fig. 5 indicates that all force spectra for building C at  $\theta = 0^\circ$  resemble gust spectra, however, when  $\theta = 90^\circ$  the acrosswind and torsional force spectra demonstrate a steep peak at a reduced frequency of 0.1. The influence of the interval between towers on spectra is not significant. It is noted from Fig. 6 and Fig. 7 that while the torsional spectra of buildings D and E at  $\theta = 0^\circ$  are analogous to gust spectra, they have a relatively broad peak at  $\theta = 90^\circ$ . The acrosswind force spectra for buildings D and E at  $\theta = 90^\circ$  show a steep peak at reduced frequencies of about 0.08-0.1. Moreover, the treatment of cutting sharp corners off decreases the peak, suggesting its influence on the separation and vortex shedding occurring on corners.

#### 4.2. Correlation between force components

It has been suggested that the correlation between alongwind and acrosswind or torsional forces is negligible for the square cross-section building (Kareem 1982). This observation is also corroborated by the study of bridge jointed twin-towered buildings. Fig. 8 shows the curves of correlation coefficients  $\rho_{xy}(\tau)$  against  $t / \delta t$  for buildings A-1 and A-2 at  $\theta = 0^\circ$  where  $\delta t$  is the sampling interval, and

$$\rho_{xy}(\tau) = \frac{R_{xy}(\tau)}{\psi_x \psi_y} \tag{18}$$

in which  $R_{xy}(\tau)$  is the correlation function between components of aerodynamic loads,  $x$  and  $y$ , and  $\psi$  is the rms value. It is noted that the correlation between the acrosswind and torsional forces is significant for all buildings in this study. The coherence between the acrosswind and torsional forces for buildings A-1 and A-2 at  $\theta = 0^\circ$  is plotted against  $nB / V_H$  in Fig. 9. It is shown that there is a dip in the coherence only for the building A-1 at the reduced frequency of 0.125 which is near the one

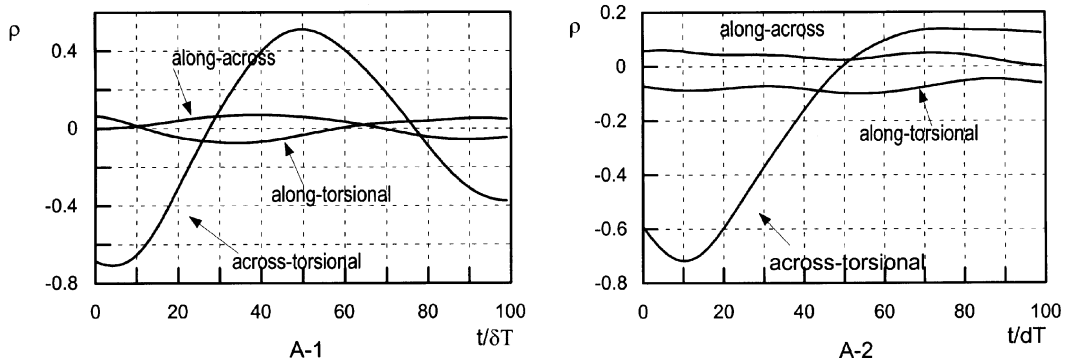


Fig. 8 Correlation coefficients for building A

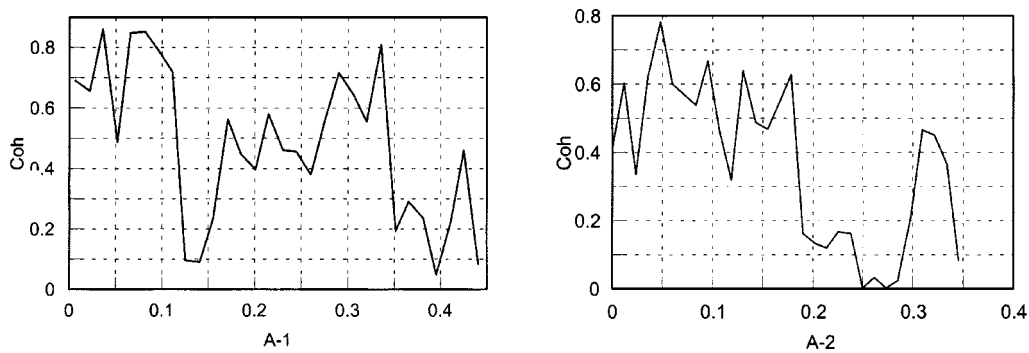


Fig. 9 Coherence between crosswind and torsional forces for building A

corresponding to the peak of the crosswind and torsional spectra of the building A-1 at  $\theta=0^\circ$  (Fig. 4).

## 5. Conclusions

The present paper is concerned with a study on the wind loads and wind excited dynamic response of bridge jointed twin-towered buildings. A series of wind tunnel tests were carried out to examine the influence of the interval between towers and the influence of plan shapes of buildings. It can be concluded that:

1. The maximum dynamic load coefficients and rms accelerations of the top floor for buildings in the study gained with the enlargement of the interval between towers within a range.
2. The acrosswind and torsional force spectra may be affected by the approach flow passing the interval due to the distortion of the vortex street.
3. The correlation between acrosswind and torsional forces is significant for all buildings under consideration.
4. The treatment, cutting sharp corners of the twin-triangular plan shape, may reduce the wind loads and wind induced dynamic response of buildings.

## Acknowledgements

The authors gratefully acknowledge the Committee of National Science Foundation of China for support of this research, provided by Grant #59895410.

## References

- Clough, R.W. and Penzien, J. (1993), *Dynamics of Structures*. Second edition. McGraw-Hill, New York.
- Islam, M.S., Ellingwood, B. and Corotis, R.B. (1990), "Dynamic response of tall buildings to stochastic wind load", *J. Struct. Div.*, ASCE, **116**(11), 2982-3002.
- Kareem, A. (1982), "Acrosswind response of buildings", *J. Struct. Div.*, ASCE, **108**(ST4), 869-887.
- Kareem, A. (1992), "Dynamic response of high-rise buildings to stochastic wind loads", *J. Wind Eng. and Ind. Aerodyn.* **41-44**, 1101-1112.
- Tschanz, T. & A.G. Davenport (1983), The base balance technique for the determination of dynamic wind loads. *J. Wind Eng. and Ind. Aerodyn.* **13**(1-3), 429-439.